The Lithographic Lens: its history and evolution

Tomoyuki Matsuyama*[a], Yasuhiro Ohmura [a], David M. Williamson [b]
[a] Precision Equipment Company, Nikon Corporation,
Kumagaya, Saitama 360-8559, Japan
[b] Nikon Research Corporation of America, 12490 N. Rancho Vistoso Blvd., Suite 130, Tucson, AZ, USA 85737

ABSTRACT

The history of Nikon's projection lens development for optical microlithography started with the first "Ultra Micro-Nikkor" in 1962, which was used for making photo-masks. Nikon's first wafer stepper "NSR-1010G" was developed with a g-line projection lens in 1980. Since then, many kinds of projection lenses have been developed for each generation of stepper or scanner. In addition to increasing numerical aperture (NA) and field size, there have been many technical transitions for the projection lens, such as shortening the wavelength, controlling Zernike aberrations with phase measurement interferometry (PMI) for low k1 lithography, using aspherical lenses, applying kinematic opto-mechanical mounts, and utilizing free asphere re-polishing steps in the lens manufacturing process. The most recent advancement in projection lens technology is liquid immersion and polarization control for high NA imaging. NA now exceeds 1.0, which is the theoretical limit for dry (in air) imaging. At each transition, the amount of information that goes through the projection lens has been increased. In this paper, the history of the microlithographic lens is reviewed from several different points of view, such as specification, optical design, lens manufacturing, etc. In addition, future options of the projection lens are discussed briefly.

Keywords: Microlithography, Projection lens, Immersion

1. INTRODUCTION

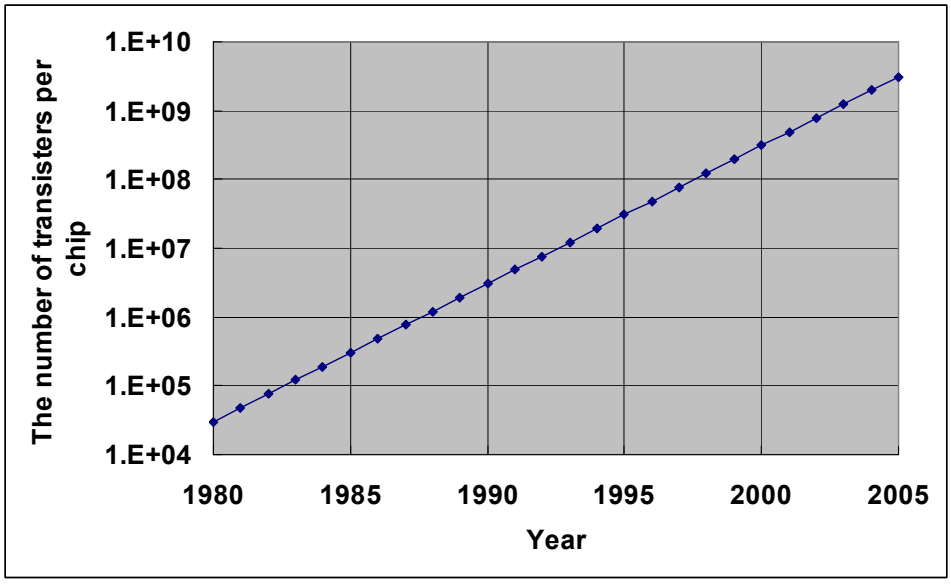

Figure 1: Trend of the number of the transistors per chip

Figure 1 indicates the trend of the number of components per chip, which had been doubling every eighteen months. This trend is called Moore's law because it was originated by Gordon Moore in 1965[1]. Although the actual number of transistors may not be exactly on this line, the line indicates the trend. To catch up with this trend, microlithographic

Optical Microlithography XIX, edited by Donis G. Flagello, Proc. of SPIE Vol. 6154
615403, (2006) · 0277-786X/06/$15 · doi: 10.1117/12.656163

lenses have been developed, which can transfer enough information to generate the required number of transistors on a chip for each generation or timing by increasing numerical aperture (NA), reducing wavelength, expanding exposure field and reducing the amount of aberration.

2. LENS SPECIFICATIONS

To explain lens performance in terms of the amount of information the lens can transfer, an extended definition of the Lagrange invariant may be convenient. The Lagrange invariant H is defined for paraxial rays in figure 1, which shows two paraxial rays through a lens[2].

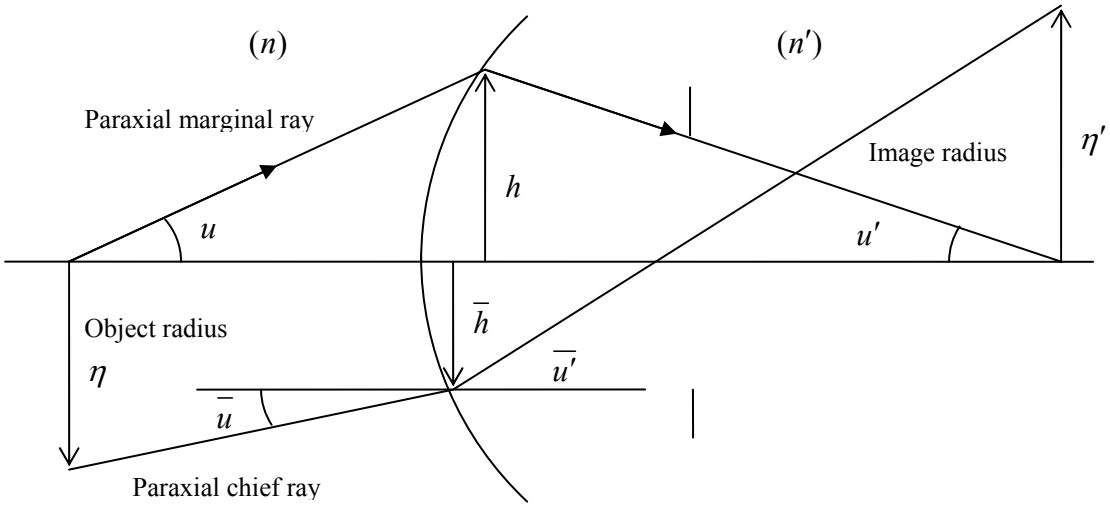

Figure 2: Two paraxial rays (marginal ray and chef ray) in an imaging lens.

$$H = n(u\bar{h} - \bar{u}h) = n'(u'\bar{h} - \bar{u}'h), \quad (1)$$

Where n is refractive index, u is paraxial marginal ray angle, h is paraxial ray height at refracting surface. A quantity associated with a chief ray is denoted by a bar, e.g., $\bar{h}$, $\bar{u}$. A primed quantity refers to the image space.

At the image surface, the paraxial marginal ray height is zero, and the chief ray height equals the image radius η'. Therefore, the Lagrange invariant simplifies to

$$H = n'u'\eta'. \quad (2)$$

The Lagrange invariant H is conserved in a lens and is one of the most important concepts in paraxial optics. The square of the Lagrange invariant is proportional to the total information transmitted by a lens. This concept may be extended to an actual projection lens. Then, the total transmitted information (*TTI*) by a lens in terms of a geometrical definition can be

$$TTI_{geometric} = (NA \cdot y_{i\max})^2, \quad (3)$$

Where, NA is numerical aperture, $y_{i\max}$ is maximum image radius.

This quantity is also one of the parameters that express a difficulty level of the optical design in terms of its specification.

Since the resolution half pitch R of a lens is defined as

$$R = \mathrm{k}_1 \frac{\lambda}{NA}, \tag{4}$$

where λ is wavelength, and k_1 is a constant process factor, the amount of total transmitted information should be inversely proportional to wavelength λ and k_1.

The total transmitted information by means of wave optics may be

$$TTI_{wave} = \left(\frac{NA \cdot y_{i\max}}{\lambda} \right)^2 . \tag{5}$$

The quantity in the brace in equation (5) expresses the intrinsic capability of a lens, defined by primary lens design specifications, including wavelength. This is because the allowable residual aberration is proportional to wavelength.

TTI_{wave} of our microlithographic lenses, which have been on the cutting edge at each time or generation, are shown in figure 3, with a notation of "TTI_wave", along with the trend of Moore's law. As we see in figure 3, the slope of the trend for TTI_{wave} is much lower than that of Moore's law. To reduce this gap, the k1 factor in equation (4) has been reduced. Reducing k1 factor has two meanings for imaging. One is to generate a finer pattern (or smaller half pitch) with lower contrast imaging, assuming the same imaging condition, such as NA, sigma, etc. In this case, the lens aberrations should be reduced, because low contrast imaging is more easily affected by aberrations. The second factor is usage of resolution enhancement techniques (RET) such as PMI, off-axis illumination, etc. to get higher contrast for a smaller half-pitch. Since the diffracted light is localized on or near the edge of the pupil for RET, aberration at the edge of pupil is more important. This also indicates that the wavefront at all positions of the pupil should be flat, since localized bumps of the wavefront, which are high order aberrations, are also not allowed. Therefore, the trend of the k1 factor indicates the trend of lens aberration level. If we take into account k1, transmitted information becomes

$$TTI_{k1} = \left(\frac{NA \cdot y_{i\max}}{\lambda \cdot k_1} \right)^2 . \tag{6}$$

The quantity in the brace in equation (6) may be recognized as the required lens performance, including specifications and lens residual aberrations. These indicate the practical difficulty level of the lens design and its manufacturing process. We may call this quantity "extended Lagrange invariant". Lens NA, maximum image height, k1 factor, and extended Lagrange invariant are shown in figure 4 (maximum image height and extended Lagrange invariant are normalized). It may be seen that the trend of the extended Lagrange invariant has been to increase exponentially. This indicates the difficulty of development of the lens, as well as the cost, which has also been increasing rapidly.

In figure 3, TTI_{k1} of our microlithographic lenses are shown with notation of "*TTI*_k1". We can still see a gap between the curve of TTI_{k1} and the trend of Moore's law, especially after 1995. This gap had been reduced by applying a scanning exposure technique. By scanning exposure of a rectangular image field, the exposure area has been expanded by a factor of approximately four. This has been allowed by the development of scanning exposure tools, along with high-power, high-repetition-rate excimer lasers. Now, the total transmitted information by a scanning exposure tool is

$$TTI_{tool} = \left(\frac{NA \cdot y_{i\max}}{\lambda \cdot k_1} \right)^2 \cdot s . \tag{7}$$

Where s is a scanning factor defined by the ratio of areas between the rectangular image field of the lens and the scanned exposure field.

The trend of TTI_{tool} is also shown in figure 3, along with the trend of our microlithographic lenses, with the notation of "TTI_k1". The remaining gap between TTI_{tool} and Moore's Law has been filled by technical innovations other than lithography.

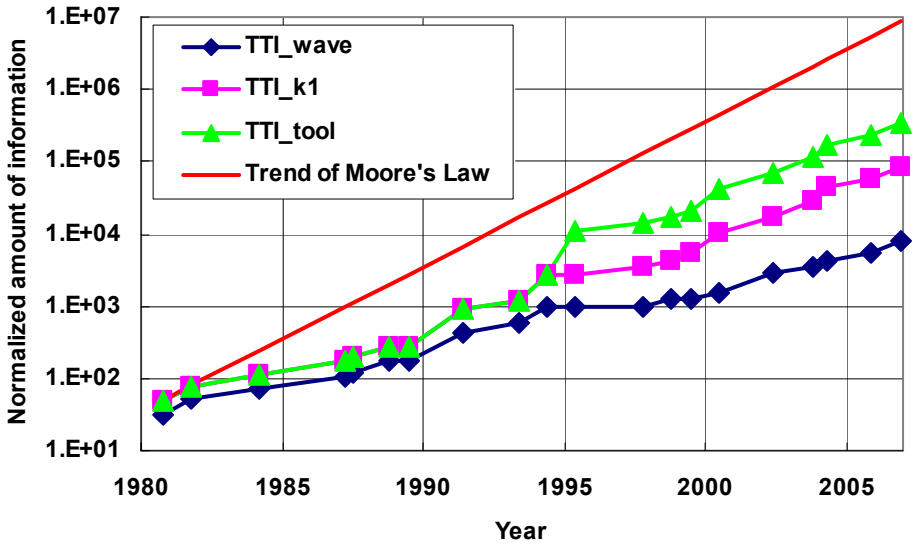

Figure 3: Trend of total transmitted information by a lens and Moore's law

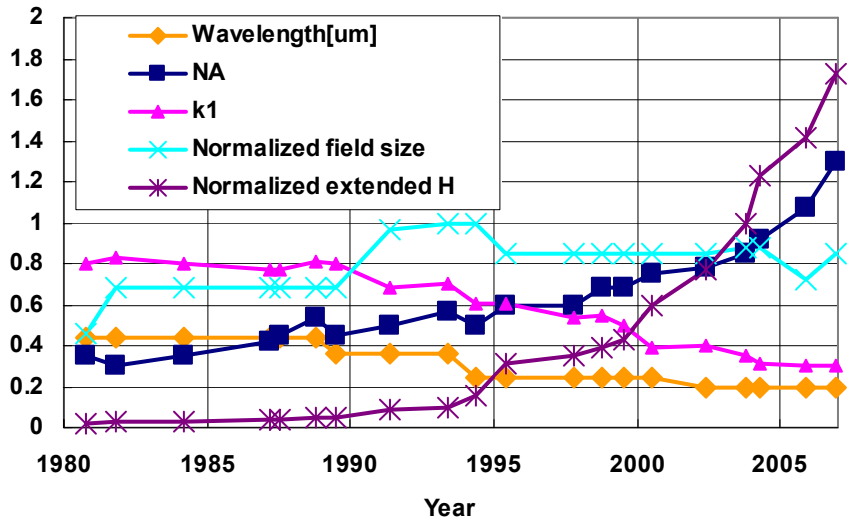

Figure 4: Trend of primary specifications and extended Lagrange invariant (H) of microlithographic lens. Field size and H are normalized.

3. OPTICAL DESIGN

Optical design of the dioptric microlithographic lens was started by modifying a design of projection lens for micro films, which was named "Ultra Micro Nikkor". This first generation microlithographic lens had a track length, or conjugate distance, of about 600mm. Maximum lens diameter was around 100mm. A design example is shown in figure 5 (a), with its primary specifications. A lens with the same specification was developed in 1981 in Nikon. In this first generation, only the wafer side was telecentric, because the magnification criterion or distortion was not so critical at that generation.

Figure 5(b) shows a typical design example for the second generation microlithographic lens. From this generation, object (reticle) side has also been telecentric. This design example was the first optical system that had all of the primary characteristics of the modern microlithographic lens, such as both side telecentric system, high NA, wide field, 1/5x-1/4x magnification, and relatively small residual aberrations. Therefore, this design became the original configuration, which is +-+-+ lens power distribution[3], for all stepper or scanner lenses, until the advent of practical utilization of large sag aspherical surfaces in the lens design. Although there were various modifications and scalings for each projection lens in each generation, the primary configuration of this design example had been continuously used since 1987.

Then, the wavelength of the microlithographic lens was moved into i-line (365nm) and field size was expanded to 17.5mm squire (figure 5 (c)) and 22mm squire (figure 5(d)). Due to the wider image field and smaller aberration criteria (due to shorter wavelength), the lens size became larger than the previous generation.

In the case of i-line or g-line, many conventional optical glass materials were used. These optical glasses have a tiny difference in refractive index between different lots or pots of glass manufacturing. (Actually, materials are manufactured by a continuously melting process, not using any pots.) The re-designing is performed for each pot (or lot) to compensate for design performance degradation due to material quantity difference from design value. Therefore, each pot design has small differences in radius of curvature of surfaces, as well as thickness of lens elements.

For i-line and g-line lens designs, not only monochromatic aberrations but also chromatic aberrations must be corrected over several nm bandwidths. This is much wider than later excimer lasers, such as Krypton Fluoride (KrF) and Argon Fluoride (ArF). Therefore, the secondary color correction was a challenge for optical designers and material developer for extraordinary dispersion glass. For wide field lens such as the example in figure 5(c), third order lateral color correction was an additional problem for the lens designer.

In contrast, a designer for deep ultra violet (DUV) lenses does not need to consider secondary color, because of the very narrow bandwidth, which is around 1pm, or sub-pm region. However, practically available lens material is limited to calcium fluoride (CaF2) and silica glass. Since these materials have relatively lower reflective indices than materials for i-line or g-line, almost the same number of lens elements and lens size were needed, because refracting power had to be split into a larger number of lens elements to achieve lower aberrations. A design example for a KrF projection lens in 1997 is shown in figure 5 (e).

For further increases of NA, practical restrictions of the size of the fused silica, and cost of the material, became issues. This brought us to utilization of a scanning exposure system. By scanning a rectangular imaging field, which has a smaller image height than the static exposure tool (stepper), 36mm x 25mm or 26mm exposure field is obtained. This technique allowed the optical designer to reduce maximum image height. The designer can use this room to increase NA. A design example in 1999 for a KrF scanning exposure tool is shown is figure 5(g). From this generation, wavefront aberration control became much more important, because of the start of low k1 lithography.

The last example in this section is a 0.75NA KrF lens with aspherical surfaces. Thanks to the use of aspherical surfaces, 0.75NA was achieved with the same size as, and shorter total track than, the previous KrF lens (0.68NA). This design uses only two aspherical surfaces and its configuration may be thought of as a modification of the second example, or a transition to the next lens type. In the most advanced ArF microlithographic lenses, several large sag aspherical surfaces were used to achieve a very large quantity of the extended Lagrange invariant. In this case, the aberration compensation concept may be different from the conventional all-spherical optical design. In the case of a conventional optical design, usually the designer tried to prevent the generation of aberrations on each surface, especially low order, and residual aberration may be compensated by aberration balancing between different surfaces. On the other hand, in the case of aspheric lens design, some aberrations remains on each surface, even for low order, and remaining aberrations are compensated by means of several aspherical surfaces. Therefore, the lens power distribution (or lens type) may be different from the conventional design, which is not allowed for conventional aberration compensation theory. Instead of generating the aberration on each surface, the lens dimension can be reduced, compared to a design without aspherical surfaces. An example of this type for 0.85NA ArF lens is shown in figure 5(h).

A photograph of two lenses is shown in figure 6. One is a lens developed in 1985 and the other is the most advanced dry lens developed in 2004. The actual lens barrel is, of course, drastically enlarged.

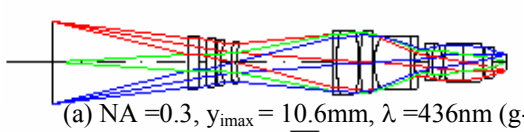

(a) NA =0.3, y_{imax} = 10.6mm, λ =436nm (g-line)

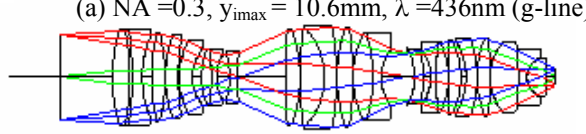

(b) NA =0.54, y_{imax} = 10.6mm, λ =436nm (g-line)

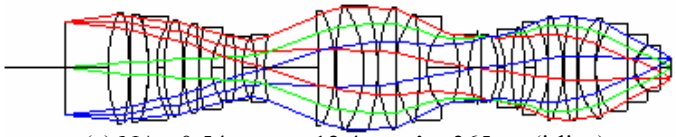

(c) NA =0.54, y_{imax} = 12.4mm, λ =365nm (i-line)

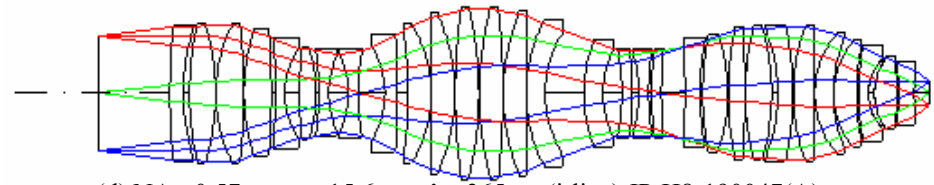

(d) NA =0.57, y_{imax} = 15.6mm, λ =365nm (i-line) JP-H8-190047(A)

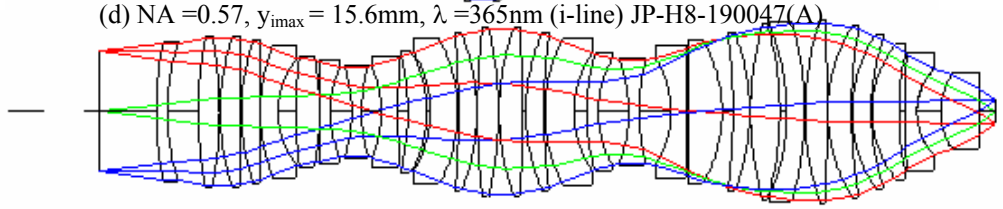

(e) NA =0.55 y_{imax} = 15.6mm, λ =248nm (KrF) JP-2000-56218(A)

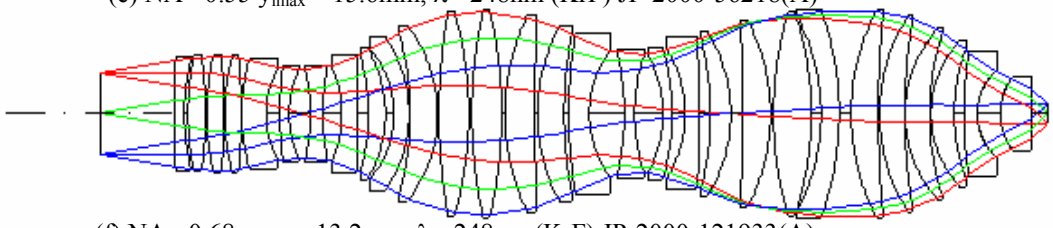

(f) NA =0.68 y_{imax} = 13.2mm, λ =248nm (KrF) JP-2000-121933(A)

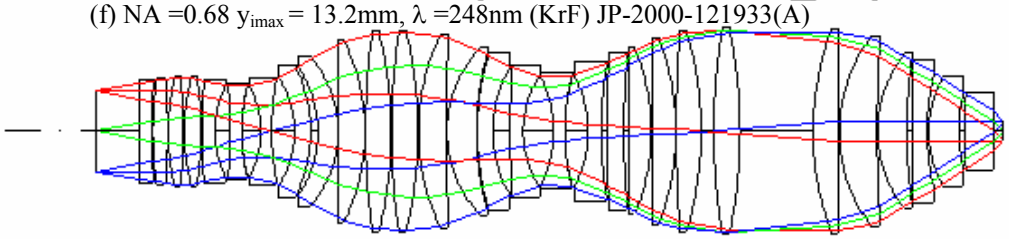

(g) NA =0.75 y_{imax} = 13.2mm, λ =248nm (KrF) JP-2000-231058(A)

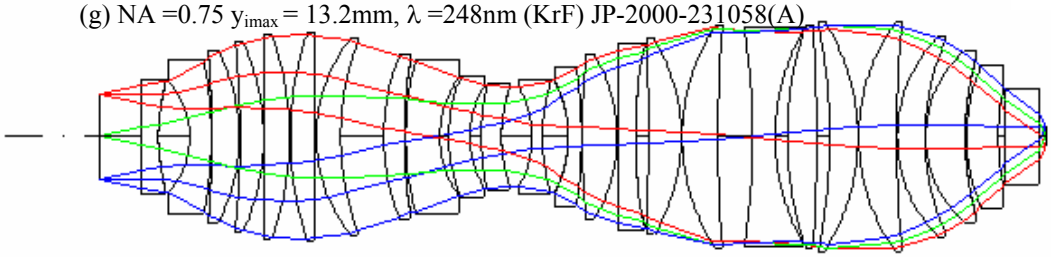

(h) NA =0.85 y_{imax} = 13.8mm, λ =193nm (ArF) JP-2004-252119(A)

Figure 5: Optical configurations of microlithographic lenses

Figure 6: Photograph of microlithographic lenses developed in 1987 (Black) and 2004 (Silver)

4. OPTOMECHANICAL DESIGN

In addition to the improvement of lens design, high lens mounting performance and its robustness are needed to make a high-performance imaging system. This is because lens element deformation due to lens mounting stresses severely degrades imaging performance.

We here briefly review the history of our lens holding mechanisms (see Fig. 7). In Nikon, a line (ring) seat has previously been used as a mount in the lens cell. The amount of peak-to-valley (P-V) lens deformation was in the sub-micron region, due to the limited processing accuracy of the ring seat, which is about 0.2 – 0.5 micron. Usually, the shape of the lens deformation was astigmatism-like, but the amount and the azimuthal angle could never be predicted. Hence, we could not predict the wavefront aberration of a lens system that used ring seat lens cells. Subsequently, three-pointed seats were used. In this case, it was possible to predict the shape and the amount of the lens deformation due to gravity. However, this three-pointed-seat generates trefoil wavefront aberration, which can not be corrected by lens element re-spacing or decentering. Consequently, the first deformation-free lens mounting was finally realized. We started to use a kinematic mounting mechanism[4] from the beginning of the low-k1 lithography generation.

A kinematic lens mounting is one of the ultimate lens mounting mechanisms, because it has high robustness against many kinds of disturbances from outside of the lens cell. A body in space has six degrees of freedom. These are translation along three axes of X, Y, Z coordinate axes (X-shift, Y-shift, Z-shift) and rotation about X, Y, Z-axes (pitching, yawing, rolling). A body is fixed when these six degrees of freedom are constrained. However if more than seven degrees of constraint are applied, the seventh constraint can be a force to deform a body. A kinematic lens mounting inhibits exactly six degrees of freedom. In other words, a kinematic lens mounting can not deform a body, because it does not have the seventh constraint. This kinematic mount is applied to our lens mounting.

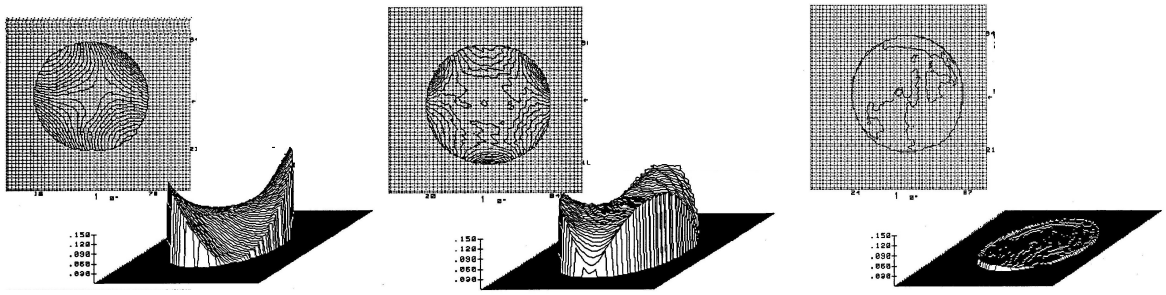

(a) Line seat lens mounting: P-V = 159nm

(b) Three pointed seat lens mounting: P-V = 159nm

(c) Kinematic lens mounting: P-V = 12nm

Figure 7: Improvement of lens mounting technology

5. LENS MANUFACTURING

As we mentioned above, improvement of aberration was needed for very low-k_1 lithography. In order to solve this challenge, our metrology capability had to be utilized most effectively in the lens manufacturing process. We developed a new conceptual lens manufacturing process, which is categorized as a differential control process, or a feedback process. In the previous DUV lens manufacturing process, aberrations due to elements' manufacturing error or assembling error could be compensated to meet the specification at that time by a lens adjusting process[5] including pre-assembly asphere re-polish, lens element orientating and positioning, as long as the error is inside of tolerance. However, metrology error, which generates higher order aberration, affects the performance of the lens even after the lens adjustment process. Final performance degradation due to the metrology error is roughly proportional to the square root of the number of measurements of element error. Therefore, a fewer number of measurements, in some senses, means an improvement of the lens performance. Figure 8 indicates a conceptual diagram of a feedback manufacturing process. At first, wavefront aberration, including distortion and defocus, are measured at multiple points across the field by a phase measurement interferometer (PMI). From the PMI data, final performance after lens adjustments is predicted. Usually, the predicted final performance is worse than the prediction from the measurement results of elements' error due to existence of the metrology error, which induces uncorrectable high order aberrations. In the next step, some lens surfaces are re-polished to generate small sag free-aspheres to compensate the residual high order aberrations due to the metrology error. In this step, control of the surface-figure change by free-asphere re-polish decides the quality of the final lens performance. The point is that only the surface figure differential between pre-re-polished surface and post-re-polished surface is important for the metrology in this process. This is a reason; this manufacturing process is categorized in differential control process. Hence, reproducibility of surface figure measurement and lens holding decide the quality of prediction of the final performance. Since a kinematic lens mount is utilized in current DUV optics, lens holding reproducibility is negligibly small. Only reproducibility of the measurement of the surfaces, which are re-polished in this process, affects the final lens performance. In addition, final performance degradation due to metrology error is drastically improved because the number of measured re-polished surface is much smaller than the total number of measured lens surfaces before initial lens assembly. As a result, lens performance degradation due to metrology error is much reduced comparing to a conventional lens manufacturing process.

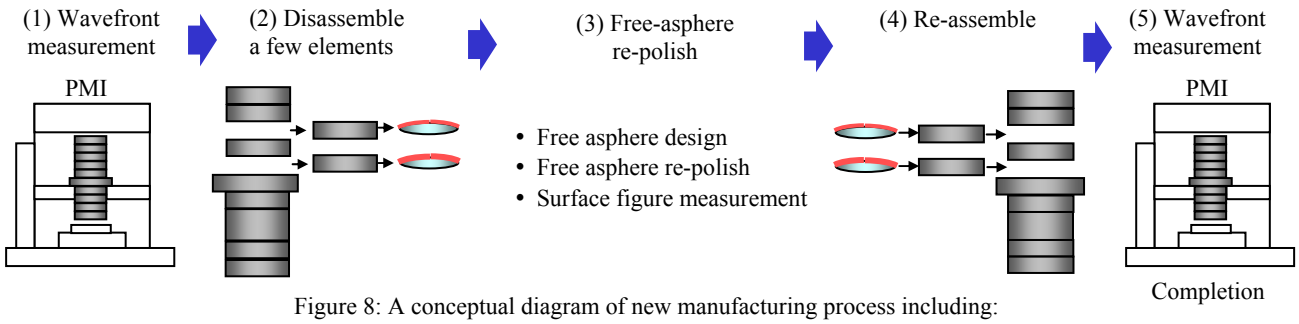

Figure 8: A conceptual diagram of new manufacturing process including:
(1) Initial wavefront measurement,
(2) Disassemble some elements,
(3) Free-asphere generation,
(4) Re-assembling, and
(5) Final wavefront measurement

Thanks to this process, the lens aberration has been drastically improved. The final lens performance for recent microlithographic lens is very close to the design value (see Fig. 9).

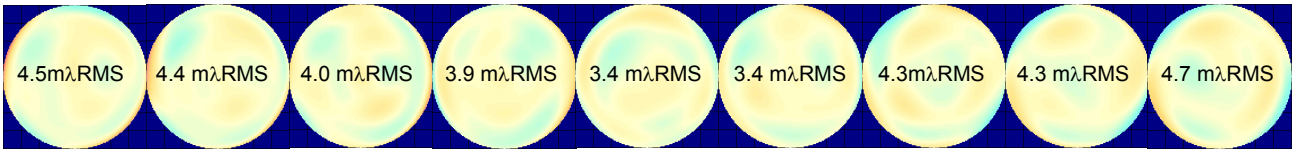

Figure 9: Scan averaged wavefront color map of 1.07NA ArF immersion lens: across the scanning slit (9 points)

6. CURRENT TOPICS OF MICROLOTHOGRAPHIC LENS

Immersion lithography is one of the hottest topics in the current microlithography industry. The concept of immersion is not new in the society of optics, because this technique has been used in microscope objective lenses for more than one hundred years. Some people have also had the idea of its application for lithography, which may be found in the patent literature [6]. However, not so many people believed the immersion technique could enter the main stream of lithography. The first trigger, which moved the lithography industry into immersion, may have been the proposal made by M. Switkes and M. Rothschild in 2002[7]. Ironically enough, the paper was a proposal for the use of immersion for F2 lithography, which has since been skipped in the current practical lithography roadmap, being replaced by ArF immersion lithography.

6.1. Optical design for immersion optics

The transition of dry microlithographic lens to wet with the same NA was not an issue for optical design because immersing water between wafer and the last surface of the lens, which is usually flat for recent lenses, only generates uniform spherical aberration (actually spherical aberration on the last surface is substantially reduced by immersion), which is easily compensated by small modification of the optical design. In other words, the same quantity of Lagrange invariant for immersion optics does not give a challenge for optical design and manufacturing so much. However, NA>1 gives rise to challenges simply because the increase of Lagrange invariant (or extended Lagrange invariant).
Merits of immersion for optical design are only two. One is a significant decrease of spherical aberration on the last surface, since the reflective index difference between glass and water is much smaller than the difference between glass and air. The other is a decrease of working distance ~10mm for dry to almost zero for immersion from the view point of lens design. These two merits, along with more aggressive use of aspherical surfaces, made it possible to design 1.0-1.07NA lenses with the same dimension as the state-of-the-art dry lens. For further increase of NA, such as 1.2, 1.3 or greater, we are introducing a catadioptric configuration. This brought us a much wider variety of optical layouts as

shown in figure 10, and the need to make a selection. Each tool vender's individual situation and strategy may result in a different selection of the lens type for NA>1.3 microlithographic lens. We have selected a relatively conservative design solution from the view point of optical design, such as the design concept shown in figure 10 (a). This design type makes it possible to get low off-axis image height, low incident angle on lens surfaces and powered mirror, and the use of a spherical mirror (no aspherical mirror).

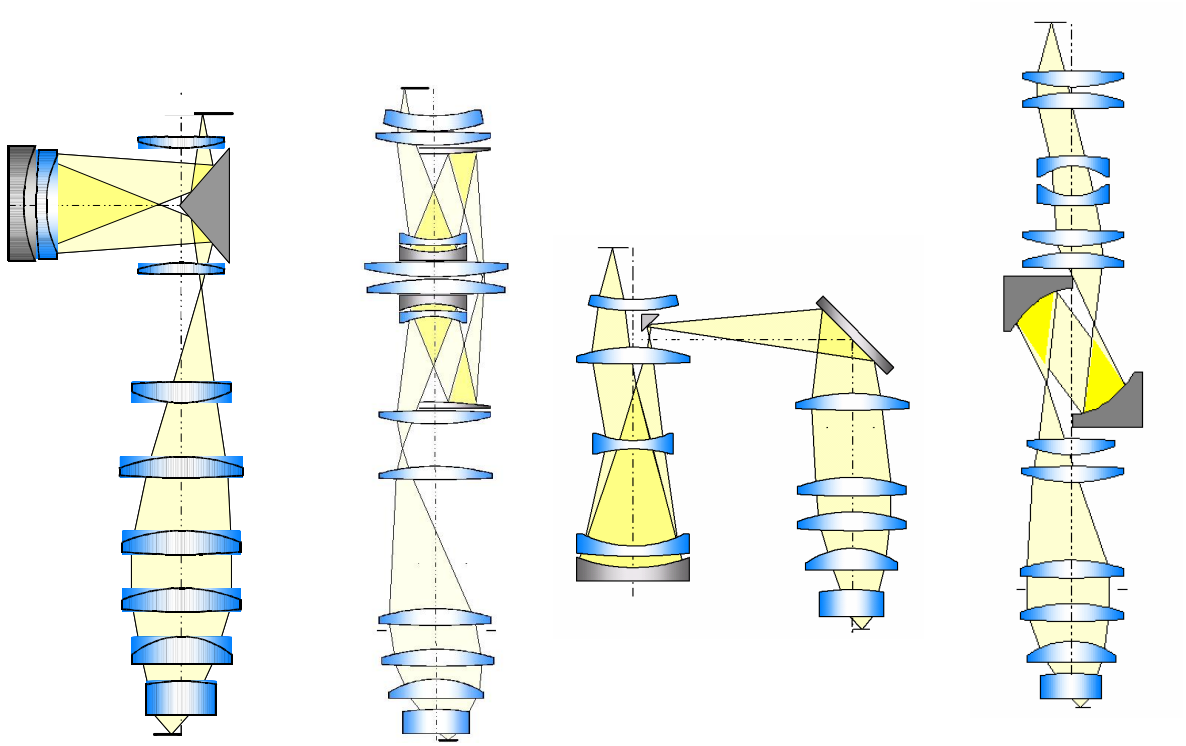

Figure 10: Variety of design concepts for catadioptric system for ArF immersion

6.2. High NA imaging

Enhancement of lens NA has an obvious impact on the resolution. Additionally, resolution enhancement technology (RET) has been used in order to achieve even higher resolution by means of controlling the illumination pupil-shape. One of the solutions is high-sigma multi pole illumination with high-NA lithography tools. In the case of high-NA imaging, polarization effects can no longer be ignored[8]. To solve this problem, a polarized illuminator[9], which supplies s-polarized light to the image plane, is necessary for high-NA lithography tools, especially immersion lithography. Figure 11 shows the effect of polarized light illumination and water immersion for 0.92NA ArF(193nm) imaging by exposure-defocus tree analysis[10] based on in-resist aerial image simulation. In this simulation, 65nmL/S pattern and dipole illumination with an outer sigma of 0.95 are assumed. Depth of focus (DOF) is defined by +/-10% critical demotion (CD) error with +/-3% mask CD error. From this simulation we can conclude as follows:

- Polarized light illumination is effective to expand dose latitude
- Effect of immersion appears in the direction of expanding DOF
- Concurrent use of immersion and polarized light illumination increases the process window significantly

Figure 12 shows measurement result of polarization status of cross-pole illumination sources on exit pupils at different field positions. Quality of illuminator polarization is quantified by ratio of specific polarization, RSP; which is defined by

$$RSP_v = \frac{I_y}{I_x + I_y} = -\frac{1}{2}\frac{S_1 - S_0}{S_0}, \quad (16)$$

and

$$RSP_h = \frac{I_x}{I_x + I_y} = \frac{1}{2}\frac{S_1 + S_0}{S_0}, \quad (17)$$

for both vertically polarized light and horizontally polarized light, respectively. Where, I_x is transmitted intensity through perfect linear-polarizer for x-axis of the pupil, I_y is transmitted intensity through perfect linear-polarizer for y-axis of the pupil, S_1 and S_0 are Stokes parameters. Fundamental RSP maximum equals 1.0. The measurement results in figure 12 confirm well high quality of the current polarized illuminator in terms of absolute value and variation across the field and across the pupil.

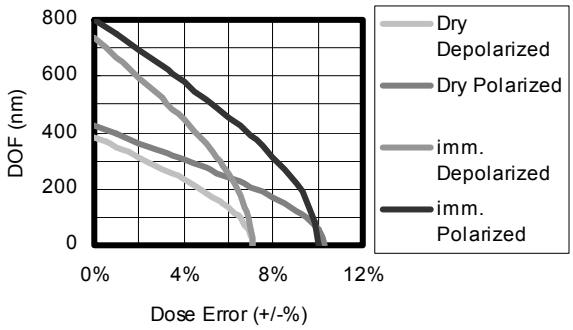

Figure 11: E-D tree analysis based on in-resist optical image simulations. Conditions are 65nmL/S, 6% aPSM, ArF (193nm), NA=0.92, Sigma=0.95, Dipole illumination. Mask error = +/-3% of CD, and CD error = +/-10%

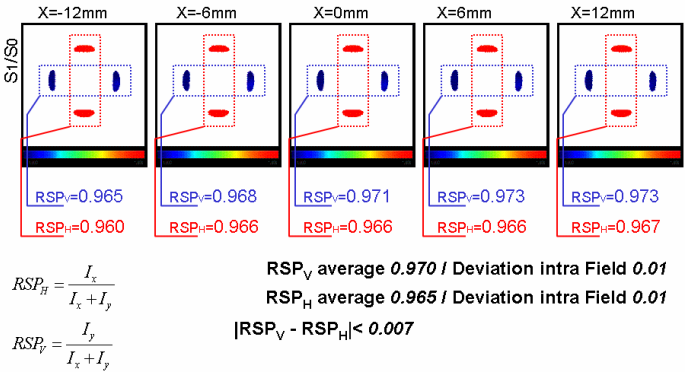

Figure 12: Polarization illumination quality of NSR-S308F, 0.92NA ArF tool, cross-pole azimuthally polarized setting

In the case of a dry system, s-polarized illumination causes a larger amount of reflectance than depolarized light on the resist surface due to Fresnel loss (approximately 10% for the 0.9 NA). This energy loss will be significantly recovered in the case of immersion (~ 1%). This is another reason why the combination of immersion and s-polarized light illumination is very effective at increasing image contrast and productivity.

6.3. Polarization aberration

As NA increases, the vector nature of the light becomes more significant for determining the imaging performance. This is not only for polarized light illumination, but also depolarized illumination imaging. Therefore, scalar wavefront aberration is no longer enough to characterize imaging performance of microlithographic lenses. Diattenuation and retardation of the lens should also be characterized and controlled. To describe an aberration function of the lens for the vector nature of the light is another topic for microlithographic lenses [11, 12]. Two major methods to characterize the lens function are, Jones matrix expression,

$$\mathbf{J}(\mathbf{p}) = \begin{pmatrix} J_{xx} & J_{xy} \\ J_{yx} & J_{yy} \end{pmatrix} \quad (18)$$

and Pauli matrix expression,

$$\mathbf{J}(\mathbf{p}) = a_0\boldsymbol{\sigma}_0 + a_1\boldsymbol{\sigma}_1 + a_2\boldsymbol{\sigma}_2 + a_3\boldsymbol{\sigma}_3 \quad (19)$$

$$\boldsymbol{\sigma}_0 = \begin{pmatrix} 1 & 0 \\ 0 & 1 \end{pmatrix} \quad \boldsymbol{\sigma}_1 = \begin{pmatrix} 1 & 0 \\ 0 & -1 \end{pmatrix} \quad \boldsymbol{\sigma}_2 = \begin{pmatrix} 0 & 1 \\ 1 & 0 \end{pmatrix} \quad \boldsymbol{\sigma}_3 = \begin{pmatrix} 0 & -i \\ i & 0 \end{pmatrix}$$

.

Though these two are physically the same, the Pauli matrix may be preferable for intuitive understanding, as well as

being easier to measure.
For both matrices, Zernike aberration expressions have been proposed recently. However, due to phase discontinuity on the pupil, a real and imaginary part expression may be necessary, instead of phase and amplitude expression for each term. This situation is different from previous scalar Zernike expression of the wavefront.

6.4. Time dependent aberration (thermal aberration) control

Time dependent aberration control such as thermal aberration became more important than before. Due to strong RET like and dipole illumination and/or combination of very small sigma illumination with PSM, intensity distribution on the pupil became stronger and more localized than conventional or annular illumination conditions and generates asymmetric temperature distribution, which causes asymmetric aberrations. Therefore, time dependent aberration change due to irradiation may not be compensated fully even using lens controller, which can change low order aberrations of the lens actively; non-negligible amount of asymmetric aberration remains. In some cases, this residual aberration causes imaging performance degradation. In order to compensate these aberrations, we have developed aberration compensation method using infrared (IR) light. IR light beam irradiation is applied to pupil lens to compensate the asymmetric temperature distribution. The amount of IR irradiation continually controlled to compensate the time dependent aberration due to exposure light irradiation.

7. FUTURE TREND OF MICROLITHOGRAPHIC LENS

Even for immersion lithography, the gap between TTI_{tool} and trend of Moore's law in figure 2 is increasing. This indicates that the challenge for the technology, even for other than lithography, is being wider and more difficult than before. Design for manufacturing[13] (DFM) may be the key technology to fill the gap. In order to make DFM more effective, the prediction accuracy of optical proximity effect (OPE) should be improved. Therefore, the following items will be topics for the imaging system on a lithography tool.

- Reduce lens aberration difference between test bench (PMI: phase measurement interferometer) and in-situ on the scanner
- Reduce aberration change due to irradiation, by means of a lens aberration controller
- Characterization of the projection lens for vector imaging simulation
- In-situ measurement of lens performance and illuminator performance

In figure 2, the horizontal axis stopped at 2007, the year when a 1.3NA immersion tool is going to be completed. The semiconductor industry may expect that higher NA such as 1.5 or 1.7 will follow after 2008. Although optical design itself is possible by extension of the current lens type for 1.3NA, assuming high index liquid and high index lens material (see figure 13), the material development for the bottom lens element has not yet been ready for the realization of such high NA tools, so far. Intrinsic birefringence of the high index crystal may be allowed to be used in the optics with limited polarization settings and pattern orientation. However, low transmittance and high temperature dependency of refractive index may not allow us to use the materials. In this situation, aggressive use of DFM or double-pitch patterning may bridge the gap until extreme ultra violet lithography (EUVL) is production-ready. We should also remember that the normalized Lagrange invariant will be 2.5 in figure 4, even for EUVL.

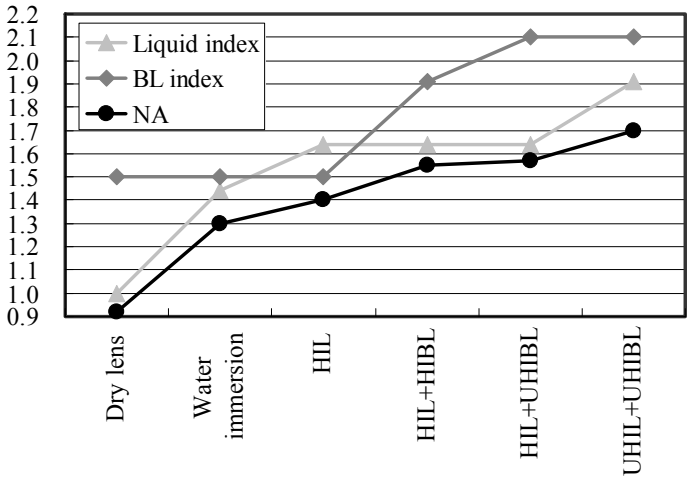

Figure 13: Feasibility study of lens design with high index materials for liquid and bottom lens. High index Liquid: HIL (n=1.64), High index bottom lens: HIBL (n = 1.91), Ultra HIL: UHIL (n = 1.82) and Ultra HIBL: UHIBL (n= 2.1)

8. SUMMARY

We introduced the concept of the extended Lagrange invariant to express difficulty of lens development. The square of the extended Lagrange invariant expresses the amount of information a microlithographic lens can transmit. As the number of transistors per chip increased according to the Moore's law, microlithographic lenses have been growing up in terms of size, increase of design parameters, utilization of aspheres, optomechanical design, and manufacturing capability to satisfy the requirement of the extended Lagrange invariant.
However, there remains a gap between the trend of the amount of information passed by the lens, and the trend of Moore's law. This gap may be filled by means of cooperation with technology improvements other than microlithographic lens development. This cooperation may be much more important than before, at least until EUVL is ready to use in a manufacturing environment.

ACKNOWLEDGEMENTS

The authors would like to thank Junichi Misawa, Hideaki Takahashi, and Toshiharu Nakashima of Nikon for helpful discussions and data supply.

REFERENCES

[1] G. Moore, "Cramming more components onto integrated circuits", Electronics, Vol. 38(8), 1965
[2] M. Kidger: *Fundamental Optical Design*, SPIE Press, 2002
[3] R. Mercado and T. Matsuyama, "Microlithographic lens", SPIE Proc. IODC Vol. 3482, 1998
[4] W.J. Smith, *Modern Optical Engineering*, 2nd ed., pp. 489-494 (McGraw-Hill, New York, New York 1990)
[5] T. Matsuyama, et al., "Improving lens performance through the most recent lens manufacturing process", SPIE Vol. 5040, 2003
[6] Y. Fukami and N. Magome : PCT/JP99/1262 (1999) WO99/49504
[7] M. Switkes and M. Rothschild: "Resolution enhancement of 157nm lithography by liquid immersion," JM3, 1 (2002) 225-228
[8] D. G. Flagello, et all, „Challenges with hyper-NA (NA>1.0) polarized light for sub l/4 resolution, Proc. SPIE Vol. 5754, 2005
[9] H. Nishinaga, et al., "Development of a polarized-light illumination and its impact", SPIE Vol. 5754, 2005
[10] B. J. Lin: "The Exposure-Defocus Forest," Jpn. J. Appl. Phys., 33 (1994) 6756-6764
[11] M. Totzeck, et all, "How to describe polarization influence on imaging", Proc. SPIE Vol. 5754, 2005

[12] G. McIntyre, et al, “Polarization Aberrations: A Comparison of Various Representations”, 2nd International Symposium on Immersion Lithography, 2005
[13] W. Staud, "Two-Way Communication", SPIE’s oemagazine, March 2005